

Advance and prospects in constraining the Yukawa-type corrections to Newtonian gravity from the Casimir effect

V. B. Bezerra,¹ G. L. Klimchitskaya,² V. M. Mostepanenko,³ and C. Romero¹

¹*Department of Physics, Federal University of Paraíba,
C.P.5008, CEP 58059-970, João Pessoa, Pb-Brazil*

²*North-West Technical University, Millionnaya St. 5, St.Petersburg, 191065, Russia*

³*Noncommercial Partnership “Scientific Instruments”,
Tverskaya St. 11, Moscow, 103905, Russia*

Abstract

We report stronger constraints on the parameters of Yukawa-type corrections to Newtonian gravity from measurements of the lateral Casimir force between sinusoidally corrugated surfaces of a sphere and a plate. In the interaction range from 1.6 to 14 nm the strengthening of previously known high confidence constraints up to a factor of 2.4×10^7 is achieved using these measurements. It is shown that the replacement of a plane plate with a corrugated one in the measurements of the normal Casimir force by means of an atomic force microscope would result in the strengthening of respective high confidence constraints on the Yukawa-type interaction by a factor of 1.1×10^{12} . The use of a corrugated plate instead of a plane plate in the experiment by means of a micromachined oscillator also leads to strengthening of the obtained constraints. We further obtain constraints on the parameters of Yukawa-type interaction from the data of experiments measuring the gradient of the Casimir pressure between two parallel plates and the gradient of the Casimir-Polder force between an atom and a plate. The obtained results are compared with the previously known constraints. The possibilities of how to further strengthen the constraints on non-Newtonian gravity are discussed.

PACS numbers: 14.80.-j, 04.50.-h, 04.80.Cc, 12.20.Fv

I. INTRODUCTION

During the last few decades possible existence of Yukawa-type corrections to Newtonian gravitational law has attracted considerable attention [1]. In the middle of eighties the problem of the so-called *fifth force* was widely discussed. Finally, no deviations from the predictions of Newtonian gravity have been found. However, after some period of time interest in hypothetical corrections to Newton's law at short separations was rekindled by numerous predictions of high energy physics beyond the Standard Model. On the one hand, many unification schemes predicted the existence of massless and light bosons such as arion [2], scalar axion [3], graviphoton [4], dilaton [5], goldstino [6], moduli [7], etc. The exchange of light bosons between two atoms belonging to different macrobodies generates an effective Yukawa-type force at short range depending on the mass of the particle. On the other hand, the Yukawa-type correction to Newton's law at submillimeter separations was predicted by multidimensional unification schemes, where additional spatial dimensions are compactified at relatively low energy of the order of 1 TeV [8–10]. In such schemes, at separations much larger than the size of a compact manifold, the gravitational potential is given by the sum of Newton's and Yukawa-type terms [11, 12]. Keeping in mind that at separations below $10\ \mu\text{m}$ the Newton's law was poorly tested experimentally, the above theoretical predictions generated considerable public excitement.

The key question is whether the Yukawa-type corrections to Newtonian gravity exist in Nature and, if they do, how strong they are and what is their interaction range. The strongest constraints on the parameters of these corrections in the interaction range larger than $4.7\ \mu\text{m}$ were obtained from the Eötvos [13, 14] and Cavendish-type [15–18] experiments. At shorter interaction range, however, the gravitational experiments do not lead to competitive constraints because the gravitational force becomes too weak. As to very short separations, the hypothetical interactions of Yukawa-type should be considered in a background of the van der Waals and Casimir forces.

The possibility of obtaining constraints on the predicted forces of Yukawa and power-type from the measurements of the Casimir force was predicted in Refs. [19, 20], respectively. The Casimir force originates from zero-point and thermal fluctuations of the electromagnetic field. It acts at separations of the order of $1\ \mu\text{m}$ between the surfaces of uncharged material bodies (see Ref. [21] for a recent overview on the subject). The modern stage in the measurement of

the Casimir force has begun in 1997 and has resulted in more than twenty experiments (see review [22]). Many of them were used to obtain constraints on the parameters of Yukawa-type interactions in the interaction range from a few nanometers to a few micrometers. In the torsion pendulum experiment [23] the constraints were obtained in Refs. [24, 25]; in the experiments using an atomic force microscope [26–28] the respective constraints were found in Refs. [29–31], and in the experiment with two crossed cylinders [32] in Ref. [33]. In all these experiments the Casimir force acting in normal direction to the surfaces of a sphere and a plate or two cylinders has been measured. As to the three dynamic experiments using a micromachined oscillator [34–36], the gradient of the normal Casimir force acting between a sphere and a plate was measured. In the proximity force approximation (PFA) this gradient is proportional to the Casimir pressure in the configuration of two parallel plates. Because of this, the respective constraints were obtained on the Yukawa-type pressure, rather than on the Yukawa-type force [34–36].

As is evident from the foregoing, the strongest constraints on the parameters of Yukawa-type corrections to Newtonian gravity at separations above a few micrometers are obtained from gravitational experiments. Within a wide interaction range from a few nanometers to a few micrometers, the strongest constraints follow from the measurement of the Casimir force. Notice that the first constraints on the Yukawa-type hypothetical interaction obtained from the Casimir effect [19, 24, 25, 29–31, 33, 34] were not as exact and reliable as the constraints obtained from the gravitational experiments at larger separations [13–18]. Specifically, for constraints of Casimir origin the confidence levels were not determined. This is due to some difficulties in the comparison between experiment and theory when the measured force is a strongly nonlinear function of separation. Later, however, the use of appropriate statistical methods [21, 22, 35] allowed to obtain from the Casimir effect the constraints of the same degree of reliability [35, 36] as from the gravitational experiments. In addition, the previously performed measurement of the Casimir force [28] was reanalyzed [37] and respective constraints valid at a 95% confidence level were obtained [36]. They are slightly weaker than those in Ref. [31], but benefit from high confidence. It is pertinent to note that a widely debated topic on the thermal contribution to the Casimir force [21, 22] is irrelevant to constraining the hypothetical forces of Yukawa-type from the Casimir effect because the difference between the alternative thermal corrections considered in the literature cannot be modeled by the Yukawa potential. As a result, the measurements of the Casimir force

have helped to strengthen the previously known constraints on the Yukawa interaction in the submicrometer range up to ten thousand times.

In this paper we obtain stronger constraints on the hypothetical interaction of Yukawa-type from recent measurement of the lateral Casimir force between sinusoidally corrugated surfaces of a sphere and a plate [38]. As compared with the previously known constraints in the interaction range below 14 nm obtained at the same high confidence (a 95% confidence level), a strengthening up to a factor of 2.4×10^7 is achieved. We also discuss respective limits on the parameters of hypothetical light elementary particles. The use of corrugated surfaces opens new prospective opportunities for constraining the Yukawa-type hypothetical interactions from the Casimir effect. In view of this fact in the present paper we propose several experiments of this type and calculate the strength of constraints that can be obtained in future in different interaction ranges. Specifically we consider the measurement of the normal Casimir force acting between a smooth sphere and a sinusoidally corrugated plate. We also explore the potentials of dynamic experiments where the separation distance between the test bodies is varied harmonically and the measured quantities are the gradients of the Casimir force [36] (Casimir-Polder force [39]), or of the Casimir pressure [40].

The structure of the paper is as follows. In Sec. II we calculate the lateral Yukawa force acting between sinusoidally corrugated surfaces of a sphere and a plate and obtain constraints on its parameters from the measurement results of Ref. [38]. Section III is devoted to the calculation of the normal Yukawa force in the configuration of a smooth sphere above a sinusoidally corrugated plate. Prospective constraints on the parameters of this force obtainable in such a configuration are presented. In Sec. IV the gradient of the Yukawa force acting between a smooth sphere and a corrugated plate in the dynamic regime is calculated and used to estimate prospective constraints. The possibility of using the gradient of the Yukawa pressure between two parallel plates in the dynamic regime for obtaining stronger constraints is considered in Sec. V. In Sec. VI the gradient of the Yukawa force in the configuration of an atom oscillating near a substrate is calculated and applied for constraining hypothetical interactions from the measurement data for the Casimir-Polder force. In Sec. VII the reader will find our conclusions and discussions.

II. STRONGER CONSTRAINTS ON THE YUKAWA-TYPE HYPOTHETICAL INTERACTION FROM THE MEASUREMENT OF THE LATERAL CASIMIR FORCE BETWEEN CORRUGATED SURFACES

It is customary to normalize the Yukawa interaction potential between two neutral point masses m_1 and m_2 (atoms) at a separation r to the potential of Newtonian gravity and represent it in the form [21, 41]

$$\frac{V^{\text{Yu}}(r)}{V^{\text{N}}(r)} = \alpha e^{-r/\lambda}, \quad V^{\text{N}}(r) = -\frac{Gm_1m_2}{r}. \quad (1)$$

Here, G is the Newtonian gravitational constant, α is a dimensionless constant characterizing the strength of the Yukawa interaction and λ is its interaction range. Specifically, if the effective Yukawa potential between atoms m_1 and m_2 is generated by the exchange of light bosons of mass m , one has $\lambda = \hbar/(mc)$.

The lateral Casimir force acting between the sinusoidally corrugated surfaces of a sphere and a plate was first experimentally demonstrated in Refs. [42, 43]. In Ref. [43] a measure of agreement between the data and the theoretically calculated lateral Casimir force was used to obtain constraints on the parameters of Yukawa interaction, namely, α and λ . This, however, did not lead to definitive constraints determined at a high confidence level because the determination of the lateral Casimir force between corrugated surfaces was not sufficiently precise.

In a recent experiment [38] the lateral Casimir force was measured between two aligned sinusoidally corrugated surfaces of a grating and a sphere with equal corrugation periods $\Lambda = 574.7$ nm and corrugation amplitudes $A_1 = 85.4$ nm and $A_2 = 13.7$ nm, respectively. The grating was made of hard epoxy with density $\rho_g = 1.08 \times 10^3$ kg/m³ on a 3 mm thick Pyrex substrate. The top of the grating was covered with a $\Delta_{\text{Au},g} = 300$ nm thick Au coating of density $\rho_{\text{Au}} = 19.28 \times 10^3$ kg/m³. The sphere of $R = 97.0$ μ m radius was made of polystyrene of density $\rho_s = 1.06 \times 10^3$ kg/m³ and uniformly coated with a $\Delta_{\text{Cr}} = 10$ nm layer of Cr ($\rho_{\text{Cr}} = 7.14 \times 10^3$ kg/m³) and then with a $\Delta_{\text{Au},s} = 50$ nm layer of Au in a thermal evaporator [38].

The lateral Casimir force was independently (without fit to any theory) measured as a function of the phase shift φ between corrugations on the sphere and on the grating over the region of separations, a , in the range from 120 to 190 nm. At each separation a_i

the maximum magnitude of the lateral Casimir force was achieved at some phase shift φ_i (keeping in mind that the dependence of the lateral force on φ is not strictly sinusoidal, φ_i must not be multiples of $\pi/2$). The absolute errors, Δ_i , of the measured maximum magnitudes of the lateral Casimir force at different separations were determined at a 95% confidence level. The measurement data were compared with the exact theory taking into account a nonzero skin depth of the Au coating and treating the Casimir force due to the nontrivial geometry of sinusoidally corrugated surfaces in the framework of the Rayleigh scattering approach. It was found that the experimental data agree with the theory within the limits of the experimental errors Δ_i . This means that the magnitudes of any possible lateral Yukawa-type force that might arise between the corrugated surfaces of a sphere and a grating must satisfy the inequality

$$|F_{ps,cor}^{Yu,lat}(a_i, \varphi_i)| \leq \Delta_i, \quad (2)$$

with Δ_i as defined above. Equation (2) follows from the fact that the measured force consisting of the lateral Casimir force and possible lateral Yukawa-type force agrees with the theoretical lateral Casimir force to within the experimental error of the force measurement (note that in the experiment under consideration the experimental errors Δ_i are much larger than the errors in computations of the lateral Casimir force with the help of the scattering approach).

To obtain constraints on the parameters of the Yukawa-type interaction α and λ , following from Eq. (2), we should substitute in this equation an explicit expression for the lateral Yukawa-type force. This can be found in the following way. We first consider a smooth homogeneous sphere of density ρ_s placed at a distance a (in the z direction) above a plane plate of density ρ_g with thickness D and linear dimension L . Under the conditions $a, \lambda \ll D, L, R$ which are satisfied in our case with large supply, one can consider a plate of infinite area and thickness (i.e., a semispace). The expression for the Yukawa-type interaction energy and force between a thick plate (semispace) and a sphere spaced at a separation a are obtained by the integration of $V^{Yu}(r)$ in Eq. (1) over both volumes and subsequently taking the negative differentiation with respect to a [30]:

$$\begin{aligned} E_{ps}^{Yu}(a) &= -4\pi^2 G\alpha\lambda^4 \rho_g \rho_s e^{-a/\lambda} \Phi(R, \lambda), \\ F_{ps}^{Yu}(a) &= -4\pi^2 G\alpha\lambda^3 \rho_g \rho_s e^{-a/\lambda} \Phi(R, \lambda), \end{aligned} \quad (3)$$

where

$$\Phi(x, \lambda) \equiv x - \lambda + (x + \lambda)e^{-2x/\lambda}. \quad (4)$$

Applying the first equality in (3) to the layer structure of the experimental test bodies, as described above, one arrives at

$$\begin{aligned} E_{ps,l}^{\text{Yu}}(a) &= -4\pi^2 G\alpha\lambda^4 e^{-a/\lambda} \Psi(\lambda), \\ \Psi(\lambda) &\equiv [\rho_{\text{Au}} - (\rho_{\text{Au}} - \rho_g)e^{-\Delta_{\text{Au},g}/\lambda}] \\ &\quad \times [\rho_{\text{Au}}\Phi(R, \lambda) - (\rho_{\text{Au}} - \rho_{\text{Cr}})\Phi(R - \Delta_{\text{Au},s}, \lambda)e^{-\Delta_{\text{Au},s}/\lambda} \\ &\quad - (\rho_{\text{Cr}} - \rho_s)\Phi(R - \Delta_{\text{Au},s} - \Delta_{\text{Cr}}, \lambda)e^{-(\Delta_{\text{Au},s} + \Delta_{\text{Cr}})/\lambda}]. \end{aligned} \quad (5)$$

As shown below, significant strengthening of constraints on α from the data of this experiment holds at λ below 10 nm. Because of this, keeping in mind that $\Delta_{\text{Au},g} = 300$ nm, not only the thickness of Pyrex substrate but the Au layer on the grating as well can be considered as infinitely thick.

Now we need to calculate the effect of aligned corrugations on the Yukawa-type energy (5). This can be done by using the method of geometrical averaging [21, 22], i.e., by replacing the closest separation a between the smooth surfaces in Eq. (5) with respective separation between corrugated surfaces and averaging over the period of corrugations. In order for such an approximate method works properly, in addition to the conditions indicated above, one more condition, namely, $\Lambda \ll R$, should be valid. It is satisfied with large supply for the listed above experimental parameters of Ref. [38].

The separation distance between the closest points of corrugated surfaces is given by

$$z_2 - z_1 = a + A_2 \sin(2\pi x/\Lambda + \varphi) - A_1 \sin(2\pi x/\Lambda). \quad (6)$$

It can be identically represented as

$$z_2 - z_1 = a + b \cos(2\pi x/\lambda - \tilde{\varphi}), \quad (7)$$

where the following notations are introduced:

$$\begin{aligned} b &\equiv b(\varphi) = (A_1^2 + A_2^2 - 2A_1A_2 \cos \varphi)^{1/2}, \\ \tan \tilde{\varphi} &= (A_2 \cos \varphi - A_1)/(A_1 \sin \varphi). \end{aligned} \quad (8)$$

Substituting Eq. (7) into Eq. (5) in place of a and performing the geometrical averaging, we arrive at

$$E_{ps,\text{cor}}^{\text{Yu}}(a, \varphi) = -4\pi^2 G\alpha\lambda^4 \Psi(\lambda) \frac{e^{-a/\lambda}}{\Lambda} \int_0^\Lambda dx e^{-b \cos(2\pi x/\Lambda - \tilde{\varphi})/\lambda}. \quad (9)$$

The integral in Eq. (9) can be calculated using the formula 2.5.40(3) in Ref. [44], with the result

$$E_{ps,cor}^{Yu}(a, \varphi) = -4\pi^2 G\alpha\lambda^4 \Psi(\lambda) e^{-a/\lambda} I_0(b/\lambda), \quad (10)$$

where $I_n(z)$ is the Bessel function of imaginary argument. The lateral Yukawa force between corrugated surfaces is obtained from Eq. (10) by taking the negative differentiation with respect to the phase shift:

$$\begin{aligned} F_{ps,cor}^{Yu,lat}(a, \varphi) &= -\frac{2\pi}{\Lambda} \frac{\partial E_{ps,cor}^{Yu}(a, \varphi)}{\partial \varphi} \\ &= 8\pi^3 G\alpha\lambda^3 \Psi(\lambda) e^{-a/\lambda} \frac{A_1 A_2}{b\Lambda} I_1(b/\lambda) \sin \varphi. \end{aligned} \quad (11)$$

Now we are in a position to determine the constraints on the parameters of the Yukawa-type interaction following from the measurement data of experiment [38]. For this purpose we substitute Eq. (11) into Eq. (2) and find the allowed values of α and λ . The computational results are shown in Fig. 1, where the allowed values of α , λ lie below the solid line and the prohibited values of α , λ lie above the solid line. These constraints were obtained in the interaction region ranging from $\lambda = 1.6$ nm to $\lambda = 35.5$ nm using the measurement data of Ref. [38] at different separations a_i . Thus, at $\lambda \leq 4.5$ nm the strongest constraints follow from Eq. (2) with $a_1 = 121.1$ nm and $\Delta_1 = 11.1$ pN. For λ in the range from 4.5 to 22.4 nm, the separation $a_2 = 124.7$ nm has been used with $\Delta_2 = 4.7$ pN. Finally, for λ from 22.4 to 35.5 nm the strongest constraints were obtained for $a_3 = 137.3$ nm and $\Delta_3 = 2.5$ pN [38].

Note that our constraints indicated by the solid line are determined with the same 95% confidence level as the absolute errors Δ_i on the right-hand side of Eq. (2). For comparison purposes in the same figure we have plotted the previously known strongest constraints on α , λ determined with 95% confidence level. The long-dashed line follows from the measurement data of the experiment [28] reanalyzed using rigorous statistical methods in Refs. [36, 37]. The short-dashed line represents constraints obtained from the experiment [36]. As can be seen in Fig. 1, our constraints indicated by the solid line are the strongest over the interaction range from 1.6 to 14 nm. The largest strengthening of previously known constraints shown by the long-dashed line by a factor of 2.4×10^7 is achieved at $\lambda = 1.6$ nm. (Note that the confidence level of slightly stronger constraints obtained in Ref. [33] from the measurement of the Casimir force between two crossed cylinders [32] cannot be determined because of several uncertainties inherent to this experiment [21, 22].) The physical reason

for so strong strengthening of the constraints obtained from the experiment with corrugated surfaces is that at a separation, for instance, $a = 121.4$ nm between the mean levels of corrugations, the distance between two closest points of the surfaces can be as small as only 22 nm.

The strongest constraints on the Yukawa-type interaction shown in Fig. 1 place limits on the parameters of gauge bosons and strange moduli [7, 45]. The existence of such particles, which are predicted in many extra-dimensional models, would result in a Yukawa-type interaction with a very large $|\alpha|$ and an interaction range λ from 10^{-8} m to 3×10^{-6} m. The obtained results can be also used to constrain the predictions of chameleon theories which introduce scalar fields with masses depending on the local background matter density [46, 47].

III. YUKAWA FORCE BETWEEN A SMOOTH SPHERE AND A CORRUGATED PLATE

The constraints on α , λ shown by the long-dashed line in Fig. 1 are obtained from the measurement of the normal Casimir force (i.e., directed perpendicular to the surface) acting between a smooth sphere and a plane plate [28]. The question arises whether the use of a corrugated plate (a grating) could lead to stronger constraints. The normal Casimir forces acting between a smooth sphere and a corrugated plate with sinusoidal [48] and rectangular [49] corrugations have been measured. However, due to the absence of sufficiently exact theory of the Casimir force applicable to corrugated surfaces at that time, it was not possible to investigate the strength of constraints which might be imposed using the results of these measurements. Presently the exact theory of the Casimir force applicable to corrugated surfaces of test bodies made of real materials, at the laboratory temperature, is available [38]. Because of this, it is pertinent to verify the potentialities of different configurations with corrugated surfaces for the strengthening of constraints on the Yukawa-type interaction. In this section we consider the configuration of a smooth sphere above a sinusoidally corrugated plate (grating).

The energy of the Yukawa-type interaction for the configuration of our interest is obtainable from Eq. (10), where the amplitude of corrugations on a sphere is put equal to zero,

$A_2 = 0$, and from Eq. (8) it follows that $b = A_1$. As a result

$$E_{p,\text{cor}}^{\text{Yu}}(a) = -4\pi^2 G\alpha\lambda^4 \Psi(\lambda) e^{-a/\lambda} I_0(A_1/\lambda). \quad (12)$$

The respective Yukawa-type force is given by

$$\begin{aligned} F_{p,\text{cor}}^{\text{Yu}}(a) &= -\frac{\partial E_{p,\text{cor}}^{\text{Yu}}(a)}{\partial a} \\ &= -4\pi^2 G\alpha\lambda^3 \Psi(\lambda) e^{-a/\lambda} I_0(A_1/\lambda). \end{aligned} \quad (13)$$

The constraints on α , λ can be found from the inequality

$$|F_{p,\text{cor}}^{\text{Yu}}(a)| \leq \Xi_F(a). \quad (14)$$

Here, the confidence interval $[-\Xi_F(a), \Xi_F(a)]$ for the difference between theoretical and mean experimental Casimir forces, $F^{\text{theor}}(a) - \bar{F}^{\text{expt}}(a)$, was found at different separations in Ref. [37] at a 95% confidence level. As an example, at separations $a = 100, 110$ and 120 nm, the half-width of the confidence interval is equal to 9.17, 8.35, and 7.96 pN, respectively.

The computations of the constraints were performed by the substitution of Eq. (13) into Eq. (14) for the realistic values of the parameters given below. The corrugated plate (grating) was precisely the same as described in Sec. II basing on the experimental configuration of Ref. [38]. The smooth polystyrene sphere of radius $R = 100 \mu\text{m}$ was assumed to be coated with only one layer of Au (as in the experiment of Ref. [28]) of thickness $\Delta_{\text{Au},s} = 100$ nm. This means that in the expression (5) for the function $\Psi(\lambda)$ one must put $\Delta_{\text{Cr}} = 0$. The obtained constraints are shown by the grey line in Fig. 2 (as in Fig. 1, the region of α , λ below the line is allowed and above the line is prohibited). For comparison purposes, we reproduce in Fig. 2 the solid and the short-dashed lines of Fig. 1, which show the constraints obtained by us in Sec. II from the measurement of the lateral Casimir force and in Ref. [36] from the experiment using a micromachined oscillator, respectively. As is seen in Fig. 2, the largest strengthening of already obtained constraints given by the solid line up to a factor of 4.5×10^4 occurs at $\lambda = 1.6$ nm. It is obtained from the measurement data at the shortest separation $a = 100$ nm.

It is instructive also to compare the prospective constraints given by the grey line in Fig. 2 with those obtained from the experiment [28] in Ref. [36] using the configuration of a smooth sphere above a plane plate (the long-dashed line in Fig. 1). Here, at $\lambda = 1.6$ nm the largest strengthening of constraints by a factor of 1.1×10^{12} is possible. So strong improvement of

the obtained constraints can be achieved due to only a replacement of the plane plate with the sinusoidally corrugated plate. The physical reason for so large strengthening is the same as in Sec. II: when the plate is corrugated the closest separation between the two surfaces is as small as 14.6 nm. This demonstrates that the use of corrugated test bodies is of high promise for obtaining stronger constraints on the Yukawa-type hypothetical interactions from the measurements of the Casimir force.

IV. GRADIENT OF THE YUKAWA FORCE BETWEEN A SMOOTH SPHERE AND A CORRUGATED PLATE IN THE DYNAMIC REGIME

The most precise experiment in Casimir physics was performed in the dynamic regime by means of micromechanical torsional oscillator [36]. This experiment exploited the configuration of a smooth sphere of $R = 150 \mu\text{m}$ radius above a plane plate which could rotate about a torsional axis. The separation distance between them was varied harmonically with the resonant frequency of the oscillator. This frequency is different in the absence and in the presence of the Casimir force $F_{sp}(a)$ between a sphere and a plate. The immediately measured quantity is the frequency shift due to the presence of the sphere which is proportional to the gradient of $F_{sp}(a)$. Using the proximity force approximation (PFA), which is valid in the experimental configuration with an accuracy of about 0.1% [21, 22], one obtains

$$P(a) = -\frac{1}{2\pi R} \frac{\partial F_{sp}(a)}{\partial a}, \quad (15)$$

where $P(a)$ is the Casimir pressure in the fictitious configuration of two plates having the same layer structure as the plate and the sphere in real experiment. In so doing, the lower plate simply coincides with the real plate. It can be replaced with a semispace if it is sufficiently thick. The upper (fictitious) plate is necessarily infinitely thick, i.e., is always a semispace. Thus, the experiment of Ref. [36] can be considered as an indirect measurement of the Casimir pressure in the configuration of two parallel plates.

The constraints on the parameters of Yukawa-type interaction in Ref. [36] were obtained from the condition

$$|P^{\text{Yu}}(a)| \leq \Xi_P(a), \quad (16)$$

where $P^{\text{Yu}}(a)$ is the Yukawa pressure in the configuration of two parallel plates and $[-\Xi_P(a), \Xi_P(a)]$ is the minimum confidence interval containing all differences between theo-

retical and mean experimental pressures, $P^{\text{theor}}(a) - \bar{P}^{\text{expt}}(a)$, within the separation region from 180 to 746 nm. This confidence interval was determined at a 95% confidence level. The use of Eq. (16) for obtaining the constraints assumes that the PFA is applicable to calculate not only the Casimir force but the Yukawa-type force as well. This applicability was confirmed in Ref. [50], where the Yukawa-type force in the experimental configuration [36] was calculated both exactly and using the PFA with coinciding results up to a 0.1% error. Thus it was shown that the PFA leads to the results of the same level of precision when applied to the Casimir and Yukawa-type forces. However, in Ref. [51] it is claimed that to obtain correct constraints on the Yukawa-type force the latter must be calculated at least ten times more precisely than the Casimir force. This claim was demonstrated to be incorrect in Ref. [52], where the constraints were reobtained without using the PFA. Instead, the inequality was used

$$\frac{1}{2\pi R} \left| \frac{\partial F_{sp}^{\text{Yu}}(a)}{\partial a} \right| \leq \Xi_P(a), \quad (17)$$

where $F_{sp}^{\text{Yu}}(a)$ is the exact Yukawa force in a sphere-plate configuration. The obtained constraints were shown to coincide with those found in Ref. [36] up to three significant figures. They are represented as the solid line in Fig. 3 (note that these constraints were already represented as short-dashed lines in Figs. 1 and 2). We emphasize that for the purpose of constraining parameters of the Yukawa-type force, it should never need to be calculated more precisely than up to 0.1% because the border of the confidence interval is determined up to only two or, at maximum, three significant figures.

Here, we check whether it is possible to strengthen the constraints of Ref. [36] by replacing a plane plate of the torsional oscillator with a corrugated plate. The parameters of the latter are assumed to be the same as in Sec. II. We perform the calculation of the prospective constraints exactly, i.e., we do not use the PFA. The Yukawa-type force acting between a smooth sphere and a corrugated plate is given by Eq. (13). Thus, for the gradient of the Yukawa force one obtains

$$\frac{\partial F_{sp}^{\text{Yu}}(a)}{\partial a} = 4\pi^2 G \alpha \lambda^2 \Psi(\lambda) e^{-a/\lambda} I_0(A_1/\lambda). \quad (18)$$

The function $\Psi(\lambda)$ is defined in Eq. (5) where in the experimental configuration of Ref. [36] $\Delta_{\text{Au},s} = 180$ nm and $\Delta_{\text{Cr}} = 10$ nm. Then, the expression for the force gradient (18) was substituted into Eq. (17). The obtained prospective constraints are shown in Fig. 3 as the

grey line. The best constraints in the interaction range $\lambda \leq 80$ nm were obtained from $\Xi_P = 3.30$ mPa at $a = 200$ nm [21, 36]. For the interaction range from 80 to 140 nm and from 140 to 250 nm the constraints shown by the grey line were obtained from $\Xi_P = 0.84$ and 0.57 mPa, as occurs at $a = 300$ and 350 nm, respectively. For comparison purposes in the same figure the long-dashed line reproduces constraints following from the experiment of Ref. [28] and reobtained in Refs. [36, 37] at a 95% confidence level. The short-dashed line shows constraints following from the so-called *Casimir-less* experiment [53] where the contribution of the Casimir force is subtracted due to the advantages of the dynamic measurement scheme. As can be seen in Fig. 3, the strengthening of constraints on the parameters of Yukawa-type interaction due to the use of corrugated plate is up to one order of magnitude. The largest strengthening (in 10 times) is achieved at $\lambda = 18.6$ nm. If we compare with the static experiment proposed in Sec. III, the use of a plate covered with sinusoidal corrugations turns out to be not so promising (one order of magnitude strengthening of constraints instead of a factor of 4.5×10^4 strengthening). This can be explained by the fact that the measurement technique using a micromachined oscillator is workable only in the region where this oscillator is linear, i.e., starting from at least two times larger separations than using an AFM. Here, the shortest separation between a corrugated plate and a smooth sphere is equal to 114.6 nm (compare with 22 nm and 14.6 nm in Secs. II and III, respectively).

V. GRADIENT OF THE YUKAWA PRESSURE BETWEEN TWO PARALLEL PLATES IN THE DYNAMIC REGIME

The only recent experiment on measuring the Casimir force which used the configuration of two parallel plates was performed in the dynamic regime [40]. The immediately measured quantity was the oscillator frequency shift due to the Casimir pressure between the plates. This frequency shift is proportional to the gradient of the Casimir pressure

$$\nu^2 - \nu_0^2 = -\beta \frac{\partial P(a)}{\partial a}, \quad (19)$$

where the coefficient is equal to $\beta \approx 0.0479$ m²/kg. Until the present time the constraints on the Yukawa-type interaction following from this experiment have not been published. Because of this, here we derive these constraints and discuss the possibilities of their strengthening.

We start with the expression for the Yukawa-type pressure between two parallel plates made of Si of density $\rho_{\text{Si}} = 2.33 \times 10^3 \text{ kg/m}^3$ and covered with chromium layers of thickness $\Delta_{\text{Cr}} = 50 \text{ nm}$, as in the experiment of Ref. [40]. Keeping in mind that the experimental parameters satisfy the conditions $a, \lambda \ll D_i, L_i$, where $D_{1,2}$ and $L_{1,2}$ are the thicknesses and linear dimensions of both plates, one can consider these plates as semispaces. The integration of the Yukawa-type potential (1) over the volumes of both plates leads to [21, 50]

$$E^{\text{Yu}}(a) = -2\pi G\alpha\lambda^3\rho_{\text{Si}}^2e^{-a/\lambda}. \quad (20)$$

Applying this equation to the plates covered with chromium layers one obtains

$$E_l^{\text{Yu}}(a) = -2\pi G\alpha\lambda^3e^{-a/\lambda} [\rho_{\text{Cr}} - (\rho_{\text{Cr}} - \rho_{\text{Si}})e^{-\Delta_{\text{Cr}}/\lambda}]^2. \quad (21)$$

This leads to the following expression for the Yukawa pressure

$$\begin{aligned} P_l^{\text{Yu}}(a) &= -\frac{\partial E_l^{\text{Yu}}(a)}{\partial a} \\ &= -2\pi G\alpha\lambda^2e^{-a/\lambda} [\rho_{\text{Cr}} - (\rho_{\text{Cr}} - \rho_{\text{Si}})e^{-\Delta_{\text{Cr}}/\lambda}]^2 \end{aligned} \quad (22)$$

and for the magnitude of its gradient

$$\left| \frac{\partial P_l^{\text{Yu}}(a)}{\partial a} \right| = 2\pi G|\alpha|\lambda e^{-a/\lambda} [\rho_{\text{Cr}} - (\rho_{\text{Cr}} - \rho_{\text{Si}})e^{-\Delta_{\text{Cr}}/\lambda}]^2. \quad (23)$$

The constraints on the Yukawa-type interaction can be obtained from the inequality

$$\beta \left| \frac{\partial P_l^{\text{Yu}}(a_i)}{\partial a} \right| \leq \Delta_i(\nu^2 - \nu_0^2), \quad (24)$$

where $\Delta_i(\nu^2 - \nu_0^2)$ is the absolute error in the measurement of the frequency shift $\nu^2 - \nu_0^2$ determined in Ref. [40] at different separations a_i where measurements were performed at a 67% confidence level. Now we substitute Eq. (23) into Eq. (24) and determine the allowed and prohibited regions of the parameters α and λ . These regions are separated by the solid line in Fig. 4. The best constraints shown by the solid line were obtained using the experimental data at different separation distances. Thus, at $\lambda \leq 0.2 \mu\text{m}$ the value $\Delta_1(\nu^2 - \nu_0^2) = 67.1 \text{ Hz}^2$ that was used occurs at $a_1 = 0.553 \mu\text{m}$. For interaction ranges from $\lambda = 0.2$ to $0.35 \mu\text{m}$ and $\lambda \geq 0.35 \mu\text{m}$ we have used the values $\Delta_2(\nu^2 - \nu_0^2) = 58.4 \text{ Hz}^2$ and $\Delta_3(\nu^2 - \nu_0^2) = 19.2 \text{ Hz}^2$, which occur at separations $a_2 = 0.574 \mu\text{m}$ and $a_3 = 0.8805 \mu\text{m}$, respectively [40]. For comparison purposes, in Fig. 4 we present also the constraints on the

Yukawa-type interaction obtained in Ref. [53] from the Casimir-less experiment (the short-dashed line) and the constraints obtained in Ref. [24] from the torsion pendulum experiment of Ref. [23] (the long-dashed line). The latter constraints will be discussed in more detail in the next section. As can be seen in Fig. 4, the constraints following from the measurement of the gradient of the Casimir pressure between two parallel plates are not as strong as the constraints obtained from previously performed experiments.

The experimental configuration of two parallel plates has some potentialities to obtain stronger constraints on the parameters of the Yukawa-type interaction. One evident resource is connected with the increase of precision [i.e., with the decrease of $\Delta_i(\nu^2 - \nu_0^2)$]. Furthermore, the replacement of Cr, as the material of metal coating, with an Au layer of the same thickness would lead to stronger constraints shown in Fig. 4 by the grey line marked 1. Moreover, the increase of thicknesses of the metal coating up to $\Delta_{\text{Au}} = 500 \text{ nm}$ would lead to even stronger constraints shown in Fig. 4 by the grey line marked 2. This line presents constraints of the same strength as those obtained in Ref. [53] from the Casimir-less experiment. Thus, the configuration of two parallel plates can be further used for obtaining constraints on the Yukawa-type interaction. As to the possibility of replacing a plane plate with a corrugated one, this does not lead to significantly stronger constraints in the experiment with parallel plates because of much larger separation distances between the test bodies.

VI. CONSTRAINTS FROM THE MEASUREMENT OF THERMAL CASIMIR-POLDER FORCE

Measurements of the Casimir-Polder force between an atom and a plate (cavity wall) and the measure of their agreement with theory provides additional opportunities for constraining the Yukawa-type corrections to Newtonian gravity. Up to now no strongest constraints have been obtained in this way, but to a large extent the potentialities of this field remain unexplored. Here, we obtain constraints on the parameters of the Yukawa-type interaction using the measurement data of dynamic experiment demonstrating the thermal Casimir-Polder force between ^{87}Rb atoms and a SiO_2 plate [39]. Rubidium atoms belonged to a Bose-Einstein condensate which was produced in a magnetic trap with frequencies equal to $\omega_{0z} = 1438.85 \text{ rad/s}$ and $\omega_{0l} = 40.21 \text{ rad/s}$ in the perpendicular and longitudinal directions to

the plate, respectively. This resulted in Thomas-Fermi radii $R_z = 2.69 \mu\text{m}$ and $R_l = 97.1 \mu\text{m}$, respectively. An oscillation amplitude $A_z = 2.50 \mu\text{m}$ in the z direction was chosen and was kept constant. By illuminating the plate with laser pulses it was possible to vary its temperature. During measurements of the Casimir-Polder force, the separation distance between the cloud of ^{87}Rb atoms and the plate was varied in the range from 7 to 11 μm . Due to the influence of the Casimir-Polder force, the oscillation frequency in the z direction shifted, and the relative frequency shift

$$\gamma_z = \frac{|\omega_{0z} - \omega_z|}{\omega_{0z}} \approx \frac{|\omega_{0z}^2 - \omega_z^2|}{2\omega_{0z}^2} \quad (25)$$

was measured as the function of the separation a between the plate and the center of mass of the condensate. The absolute errors in the measurement of γ_z at different separations a_i , $\Delta_i\gamma_z$, were found in Ref. [39] at a 67% confidence level.

The Yukawa-type interaction (if any) would also lead to some frequency shift in the perpendicular direction to the plate. It can be calculated in the following way. The Yukawa energy of a single atom of mass m_1 above a thick plate can be found by the integration of the potential (1) over the volume of the plate

$$E_{ap}^{\text{Yu}}(a) = -2\pi G\alpha\lambda^2 m_1 \rho_2 e^{-a/\lambda}, \quad (26)$$

where $\rho_2 = 2.203 \times 10^3 \text{ kg/m}^3$ is the density of plate material (fused silica). From this the Yukawa-type force acting on an atom is given by

$$F_{ap}^{\text{Yu}}(a) = -\frac{\partial E_{ap}^{\text{Yu}}(a)}{\partial a} = -2\pi G\alpha\lambda m_1 \rho_2 e^{-a/\lambda}. \quad (27)$$

The frequency shift due to the Yukawa force (27) can be calculated by averaging over the deviations of separate atoms in the z -direction from the center of mass of a condensate, which is taken at the origin of the z axis, and over the oscillation period [21, 54, 55]

$$\begin{aligned} \omega_{0z}^2 - \omega_z^2 &= -\frac{\omega_{0z}}{\pi A_z m_1} \int_0^{2\pi/\omega_{0z}} d\tau \cos(\omega_{0z}\tau) \\ &\times \int_{-R_z}^{R_z} dz n_z(z) F_{ap}^{\text{Yu}}[a + z + A_z \cos(\omega_{0z}\tau)]. \end{aligned} \quad (28)$$

Here, the distribution function of the atomic gas density is given by

$$n_z(z) = \frac{15}{16R_z} \left(1 - \frac{z^2}{R_z^2}\right)^2. \quad (29)$$

Substituting Eq. (27) into Eq. (28) we can find the relative frequency shift due to the Yukawa-type interaction defined in the same way as in Eq. (25)

$$\begin{aligned} \gamma_z^{\text{Yu}}(a) &= \frac{G\alpha\lambda\rho_2}{\omega_{0z}A_z} \frac{15}{16R_z} e^{-a/\lambda} \int_{-R_z}^{R_z} dz \left(1 - \frac{z^2}{R_z^2}\right)^2 e^{-z/\lambda} \\ &\times \int_0^{2\pi/\omega_{0z}} d\tau \cos(\omega_{0z}\tau) e^{-A_z \cos(\omega_{0z}\tau)/\lambda}. \end{aligned} \quad (30)$$

Calculating both integrals on the right-hand side of Eq. (30), one obtains [44]

$$\gamma_z^{\text{Yu}}(a) = \frac{15\pi G\lambda\rho_2}{8\omega_{0z}^2 A_z} \alpha e^{-a/\lambda} \Theta\left(\frac{R_z}{\lambda}\right) I_1\left(\frac{A_z}{\lambda}\right), \quad (31)$$

where

$$\Theta(t) \equiv \frac{16}{t^5} [t^2 \sinh(t) - 3t \cosh(t) + 3 \sinh(t)]. \quad (32)$$

The constraints on the parameters of Yukawa-type interaction can be now obtained from the inequality

$$|\gamma_z^{\text{Yu}}(a_i)| \leq \Delta_i \gamma_z, \quad (33)$$

where the left-hand side is defined in Eq. (31). The computational results are presented by the solid line in Fig. 5. Within the interaction range $\lambda \leq 2 \mu\text{m}$ the best constraints given by the solid line were obtained in an equilibrium situation when the temperatures of the plate and of the environment are equal to 310 K. In so doing the magnitude of the absolute error $\Delta_1 \gamma_z = 3.06 \times 10^{-5}$ was used which occurs at the separation distance $a_1 = 6.88 \mu\text{m}$ [39]. Within the interaction range $\lambda \geq 5 \mu\text{m}$ the best constraints are also obtained in an equilibrium situation. Here, the measurement at the separation $a_2 = 9.95 \mu\text{m}$ was used with the respective absolute error equal to $\Delta_2 \gamma_z = 1.41 \times 10^{-5}$ [39]. In an intermediate interaction range of λ from 2 to $5 \mu\text{m}$ the best constraints follow from out of equilibrium measurement data, where the temperature of an environment was the same as before, but the temperature of the plate was equal to 479 K. The best constraints were found from the measurement performed at $a_3 = 7.44 \mu\text{m}$ with $\Delta_3 \gamma_z = 2.35 \times 10^{-5}$ [39].

For comparison purposes, the long-dashed line in Fig. 5 shows the constraints obtained in Ref. [24] from the torsion pendulum experiment of Ref. [23]. It is seen that constraints obtained from the torsion pendulum experiment are from about one to two orders of magnitude stronger (depending on the interaction range) than the constraints given by the solid line. It is important to bear in mind, however, that the constraints from the measurement of the Casimir-Polder force (the solid line) were determined at a 67% confidence level, whereas

the confidence level of constraints given by the long-dashed line cannot be determined. This is caused by some uncertain features of the experiment [23] discussed in Refs. [21, 22]. The short-dashed line in Fig. 5 presents the strongest constraints in this interaction range following from gravitational experiments. These are high confidence constraints obtained in Ref. [17]. A new experimental technique suited for obtaining stronger constraints on the Yukawa-type interaction from the measurements of the Casimir-Polder force is discussed in Ref. [56].

Recently one more determination of the limits on the Yukawa-type interaction in the range of about $1\ \mu\text{m}$ from the measurement of the Casimir force using a torsion balance has been reported [57]. In this experiment a glass plate and a spherical lens of $R = 20.7\ \text{cm}$ radius were used as the test bodies, both coated with a 20 nm Cr layer and then with a $1\ \mu\text{m}$ layer of Au. This experiment is not an independent measurement of the Casimir force, like experiments in Refs. [26–28, 34–36], because the measurement data for the gradient of the force were fitted to the sum of two functions: the gradient of the expected electrostatic force and the gradient of the Casimir force taking into account the conductivity and roughness effects. To obtain the limits on α , the fit to the sum of three functions was performed with inclusion of the Yukawa-type force and λ as an additional fitting parameter. The Yukawa-type force was calculated using the results of Ref. [24]. The obtained limits determined at a 95% confidence level are shown as the grey line in Fig. 5. As can be seen in Fig. 5, these limits are a bit stronger than the limits obtained from the measurement of the Casimir-Polder force (the solid line), but much weaker than the limits shown by the long-dashed line which are obtained [24] from the measurement data of Ref. [23]. The authors of Ref. [57] note, however, that the accuracy of the experiment [23] was overestimated and compare their limits not with the results of Ref. [24], but with the results of Ref. [25] where much weaker constraints from the same measurement data [23] were found. From this they conclude that their limits are stronger than those obtained on the basis of Ref. [23]. It seems that this conclusion is not well justified. The point is that Ref. [24] had already taken into account that the accuracy of the experiment [23] was overestimated (this is discussed in [24] in detail). The difference between the constraints obtained in Refs. [24] and [25] using the same data of Ref. [23] is explained by the fact that in [24] the corrections due to the surface roughness, finite conductivity of the boundary metal and nonzero temperature were taken into account, whereas in [25] they were disregarded. Thus, in fact the constraints of Ref. [57] are weaker

than those following from the measurements of Ref. [23]. The advantage of the constraints of Ref. [57] is that they are obtained at a high confidence level, whereas the confidence level of the constraints obtained from the data of Ref. [23] cannot be determined on a solid basis.

VII. CONCLUSIONS AND DISCUSSION

In the foregoing we have considered constraints on the Yukawa-type corrections to Newtonian gravity in micrometer and submicrometer interaction ranges following from the measurements of the Casimir and Casimir-Polder forces. This field of research has already received wide recognition as an important adjunct to the gravitational experiments of Eötvös and Cavendish-type. Novel constraints on the parameters of Yukawa-type interactions from the Casimir effect were obtained at a high confidence level and were used for constraining masses of predicted light elementary particles and other parameters of the theory of fundamental interactions beyond the Standard Model [58].

In this paper we have analyzed several experiments on measuring the Casimir and Casimir-Polder force which were not used up to date for constraining corrections to Newtonian gravity. The most striking result obtained above is that recent experiment on measuring the lateral Casimir force between corrugated surfaces of a sphere and a plate [38] leads to a great strengthening of the previously known high confidence constraints up to a factor of 2.4×10^7 . The constraints obtained from this experiment are shown to be the strongest in the interaction range from 1.6 to 14 nm. This raises a question on the role of corrugated surfaces in other experimental configurations used to obtain constraints on the parameters of Yukawa-type interactions.

The influence of sinusoidal corrugations on the Yukawa force was calculated above by using the approximate method of geometrical averaging. This method is applicable under several conditions which are well satisfied for the experimental configurations considered in the paper. In fact, the geometrical averaging works better for the Yukawa force than for the Casimir force. The point is that the Yukawa force is static and is not influenced by the diffraction-type effects which are essential for the Casimir force (the better applicability of the geometrical averaging to the electrostatic than to the Casimir force was also noted in Ref. [38]). We have shown that the replacement of a plane plate with a sinusoidally corrugated plate in the experiment on measuring the normal Casimir force in a sphere-plate

configuration [28] would strengthen the constraints obtained from the measurement data of Ref. [28] in Ref. [36] by a factor of 1.1×10^{12} .

Next, we have obtained constraints on the Yukawa-type interaction from the measurement data of the dynamic experiment using a micromechanical torsional oscillator [36] when the plane plate is replaced with the corrugated one. It was shown that up to an order of magnitude strengthening is achievable in this way in comparison with the previously obtained constraints.

We have also obtained constraints from the measurement data of two dynamic experiments which were not used previously for constraining the Yukawa-type interaction. These are the measurement of the gradient of the Casimir pressure in the configuration of two parallel plates [40] and of the gradient of the thermal Casimir-Polder force between an atom and a dielectric plate [39]. For the parallel plate experiment, the obtained constraints are weaker than those obtained from other experiments, but they can be significantly strengthened by replacing a Cr metal coating with a thicker Au coating. For the experiment dealing with the Casimir-Polder interaction, a frequency shift of the condensate oscillating due to the presence of Yukawa-type interaction was found. It was shown that the obtained constraints are weaker than those found in Ref. [24] from the torsion pendulum experiment [23]. It was also shown that the constraints following from the measurement of the Casimir-Polder interaction are of almost the same strength as the constraints obtained in recent experiment [57]. For both the experiment with two parallel plates and the measurement of the Casimir-Polder force, the replacement of a plane plate with a grating does not lead to a notable improvement in the strength of constraints because of the relatively large separation distances between the test bodies in these experiments.

Thus, we have shown that the use of the measurement data of recent experiment on the lateral Casimir force leads to more than seven orders of magnitude strengthening in the previously obtained constraints. We have demonstrated that even higher promise is expected from the measurement of the normal Casimir force by means of an AFM if the plane plate were replaced with a corrugated plate. These results and the analysis of some other experiments confirm prospective future trends for obtaining stronger constraints on non-Newtonian gravity from the measurement of both the Casimir and Casimir-Polder forces.

Acknowledgments

The authors thank FAPES-ES/CNPq (PRONEX) for partial financial support. G.L.K. and V.M.M. are grateful to the Federal University of Paraíba (João Pessoa, Brazil), where this work was performed, for kind hospitality. V.B.B. and C.R. also thank CNPq for partial financial support.

-
- [1] E. Fischbach and C. L. Talmadge, *The Search for Non-Newtonian Gravity* (Springer, New York, 1999).
 - [2] A. A. Anselm and N. G. Uraltsev, *Phys. Lett. B* **114**, 39 (1982).
 - [3] R. D. Peccei and H. R. Quinn, *Phys. Rev. Lett.* **38**, 1440 (1977).
 - [4] S. Ferrara, J. Scherk, and B. Zumino, *Nucl. Phys. B* **121**, 393 (1977).
 - [5] Y. Fujii, *Int. J. Mod. Phys. A* **6**, 3505 (1991).
 - [6] S. Deser and B. Zumino, *Phys. Rev. Lett.* **38**, 1433 (1977).
 - [7] S. Dimopoulos and G. F. Giudice, *Phys. Lett. B* **379**, 105 (1996).
 - [8] I. Antoniadis, N. Arkani-Hamed, S. Dimopoulos, and G. Dvali, *Phys. Lett. B* **436**, 257 (1998).
 - [9] N. Arkani-Hamed, S. Dimopoulos, and G. Dvali, *Phys. Lett. B* **429**, 263 (1998).
 - [10] N. Arkani-Hamed, S. Dimopoulos, and G. Dvali, *Phys. Rev. D* **59**, 086004 (1999).
 - [11] E. G. Floratos and G. K. Leontaris, *Phys. Lett. B* **465**, 95 (1999).
 - [12] A. Kehagias and K. Sfetsos, *Phys. Lett. B* **472**, 39 (2000).
 - [13] S. Schlamminger, K.-Y. Choi, T. A. Wagner, J. H. Gundlach, and E. G. Adelberger, *Phys. Rev. Lett.* **100**, 041101 (2008).
 - [14] G. L. Smith, C. D. Hoyle, J. H. Gundlach, E. G. Adelberger, B. R. Heckel, and H. E. Swanson, *Phys. Rev. D* **61**, 022001 (2000).
 - [15] J. K. Hoskins, R. D. Newman, R. Spero, and J. Schultz, *Phys. Rev. D* **32**, 3084 (1985).
 - [16] D. J. Kapner, T. S. Cook, E. G. Adelberger, J. H. Gundlach, B. R. Heckel, C. D. Hoyle, and H. E. Swanson, *Phys. Rev. Lett.* **98**, 021101 (2007).
 - [17] S. J. Smullin, A. A. Geraci, D. M. Weld, J. Chiaverini, S. Holmes, and A. Kapitulnik, *Phys. Rev. D* **72**, 122001 (2005).
 - [18] D. M. Weld, J. Xia, B. Cabrera, and A. Kapitulnik, *Phys. Rev. D* **77**, 062006 (2008).

- [19] V. A. Kuzmin, I. I. Tkachev, and M. E. Shaposhnikov, Pis'ma v ZhETF **36**, 49 (1982) [JETP Lett. **36**, 59 (1982)].
- [20] V. M. Mostepanenko and I. Yu. Sokolov, Phys. Lett. A **125**, 405 (1987).
- [21] M. Bordag, G. L. Klimchitskaya, U. Mohideen, and V. M. Mostepanenko, *Advances in the Casimir Effect* (Oxford University Press, Oxford, 2009).
- [22] G. L. Klimchitskaya, U. Mohideen, and V. M. Mostepanenko, Rev. Mod. Phys. **81**, 1827 (2009).
- [23] S. K. Lamoreaux, Phys. Rev. Lett. **78**, 5 (1997); **81**, 5475(E) (1998).
- [24] M. Bordag, B. Geyer, G. L. Klimchitskaya, and V. M. Mostepanenko, Phys. Rev. D **58**, 075003 (1998).
- [25] J. C. Long, H. W. Chan, and J. C. Price, Nucl. Phys. B **539**, 23 (1999).
- [26] U. Mohideen and A. Roy, Phys. Rev. Lett. **81**, 4549 (1998).
- [27] A. Roy, C.-Y. Lin, and U. Mohideen, Phys. Rev. D **60**, 111101(R) (1999).
- [28] B. W. Harris, F. Chen, and U. Mohideen, Phys. Rev. A **62**, 052109 (2000).
- [29] M. Bordag, B. Geyer, G. L. Klimchitskaya, and V. M. Mostepanenko, Phys. Rev. D **60**, 055004 (1999).
- [30] M. Bordag, B. Geyer, G. L. Klimchitskaya, and V. M. Mostepanenko, Phys. Rev. D **62**, 011701(R) (2000).
- [31] E. Fischbach, D. E. Krause, V. M. Mostepanenko, and M. Novello, Phys. Rev. D **64**, 075010 (2001).
- [32] T. Ederth, Phys. Rev. A **62**, 062104 (2000).
- [33] V. M. Mostepanenko and M. Novello, Phys. Rev. D **63**, 115003 (2001).
- [34] R. S. Decca, E. Fischbach, G. L. Klimchitskaya, D. E. Krause, D. López, and V. M. Mostepanenko, Phys. Rev. D **68**, 116003 (2003).
- [35] R. S. Decca, D. López, E. Fischbach, G. L. Klimchitskaya, D. E. Krause, and V. M. Mostepanenko, Ann. Phys. (N.Y.) **318**, 37 (2005).
- [36] R. S. Decca, D. López, E. Fischbach, G. L. Klimchitskaya, D. E. Krause, and V. M. Mostepanenko, Phys. Rev. D **75**, 077101 (2007); Eur. Phys. J. C **51**, 963 (2007).
- [37] G. L. Klimchitskaya, U. Mohideen, and V. M. Mostepanenko, J. Phys. A: Math. Theor. **40**, F339 (2007).
- [38] H.-C. Chiu, G. L. Klimchitskaya, V. N. Marachevsky, V. M. Mostepanenko, and U. Mohideen,

- Phys. Rev. B **80**, 121402(R) (2009).
- [39] J. M. Obrecht, R. J. Wild, M. Antezza, L. P. Pitaevskii, S. Stringari, and E. A. Cornell, Phys. Rev. Lett. **98**, 063201 (2007).
- [40] G. Bressi, G. Carugno, R. Onofrio, and G. Ruoso, Phys. Rev. Lett. **88**, 041804 (2002).
- [41] E. G. Adelberger, B. R. Heckel, and A. E. Nelson, Ann. Rev. Nucl. Part. Sci. **53**, 77 (2003).
- [42] F. Chen, U. Mohideen, G. L. Klimchitskaya, and V. M. Mostepanenko, Phys. Rev. Lett. **88**, 101801 (2002).
- [43] F. Chen, U. Mohideen, G. L. Klimchitskaya, and V. M. Mostepanenko, Phys. Rev. A **66**, 032113 (2002).
- [44] A. P. Prudnikov, Yu. A. Brychkov, and O. I. Marichev, *Integrals and Series. Vol. 1* (Gordon and Breach, New York, 1986).
- [45] S. Dimopoulos and A.A. Geraci, Phys. Rev. D **68**, 124021 (2003).
- [46] Ph. Brax, C. van de Bruck, A.-C. Davis, D. F. Mota, and D. Shaw, Phys. Rev. D **76**, 124034 (2007).
- [47] D. F. Mota and D. Shaw, Phys. Rev. D **75**, 063501 (2007).
- [48] A. Roy and U. Mohideen, Phys. Rev. Lett. **82**, 4380 (1999).
- [49] H. B. Chan, Y. Bao, J. Zou, R. A. Cirelli, F. Klemens, W. M. Mansfield, and C. S. Pai, Phys. Rev. Lett. **101**, 030401 (2008).
- [50] R. S. Decca, E. Fischbach, G. L. Klimchitskaya, D. E. Krause, D. López, and V. M. Mostepanenko, Phys. Rev. D **79**, 124021 (2009).
- [51] D. A. R. Dalvit and R. Onofrio, Phys. Rev. D **80**, 064025 (2009).
- [52] E. Fischbach, G. L. Klimchitskaya, D. E. Krause, and V. M. Mostepanenko, arXiv:0911.1950.
- [53] D. E. Krause, R. S. Decca, D. López, and E. Fischbach, Phys. Rev. Lett. **98**, 050403 (2007).
- [54] M. Antezza, L. P. Pitaevskii, and S. Stringari, Phys. Rev. A **70**, 053619 (2004).
- [55] G. L. Klimchitskaya and V. M. Mostepanenko, J. Phys. A: Math. Theor. **41**, 312002(F) (2008).
- [56] F. Sorrentino, A. Alberti, G. Ferrari, V. V. Ivanov, N. Poli, M. Schioppo, and G. M. Tino, Phys. Rev. A **79**, 013409 (2009).
- [57] M. Masuda and M. Sasaki, Phys. Rev. Lett. **102**, 171101 (2009).
- [58] Particle Data Group, Phys. Lett. B **667**, 1 (2008).

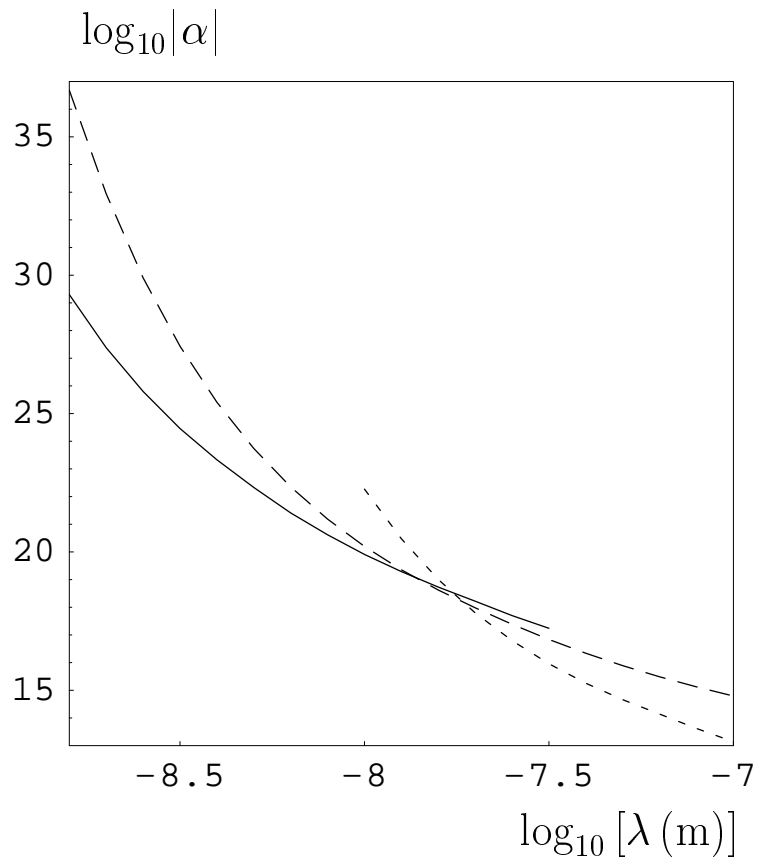


FIG. 1: Constraints on the parameters of Yukawa-type interaction from measurements of the lateral Casimir force between corrugated surfaces (the solid line), and from measurements of the normal Casimir force by means of an atomic force microscope (the long-dashed line), and a micromachined oscillator (the short-dashed line). The allowed regions in the (λ, α) -plane lie beneath the lines.

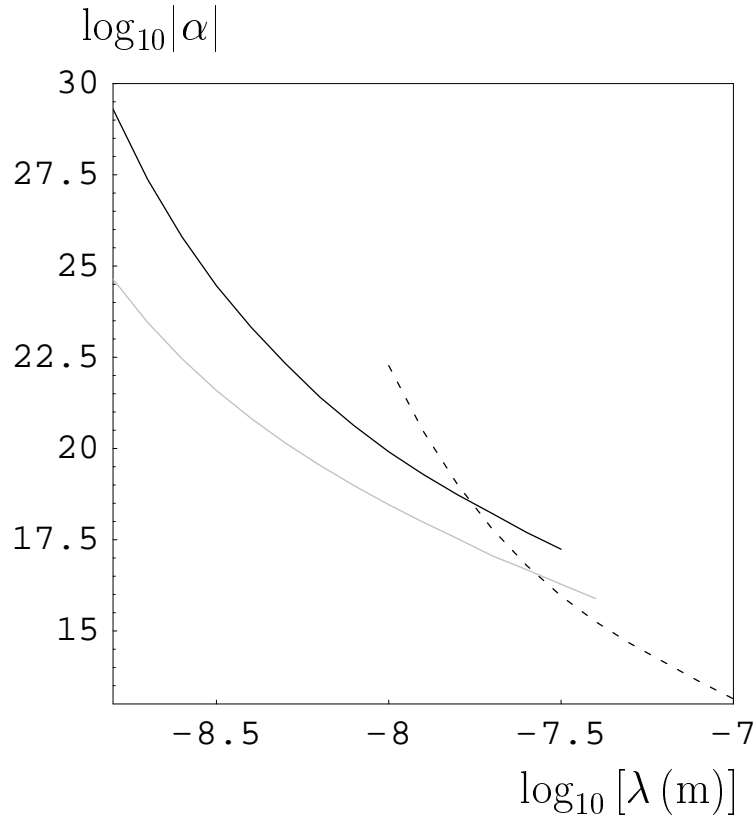


FIG. 2: Constraints on the parameters of Yukawa-type interaction from proposed measurements of the normal Casimir force between a smooth sphere and a corrugated plate (the grey line), from measurements of the lateral Casimir force between corrugated surfaces (the solid line), and from measurements of the normal Casimir force using a micromachined oscillator (the short-dashed line). The allowed regions in the (λ, α) -plane lie beneath the lines.

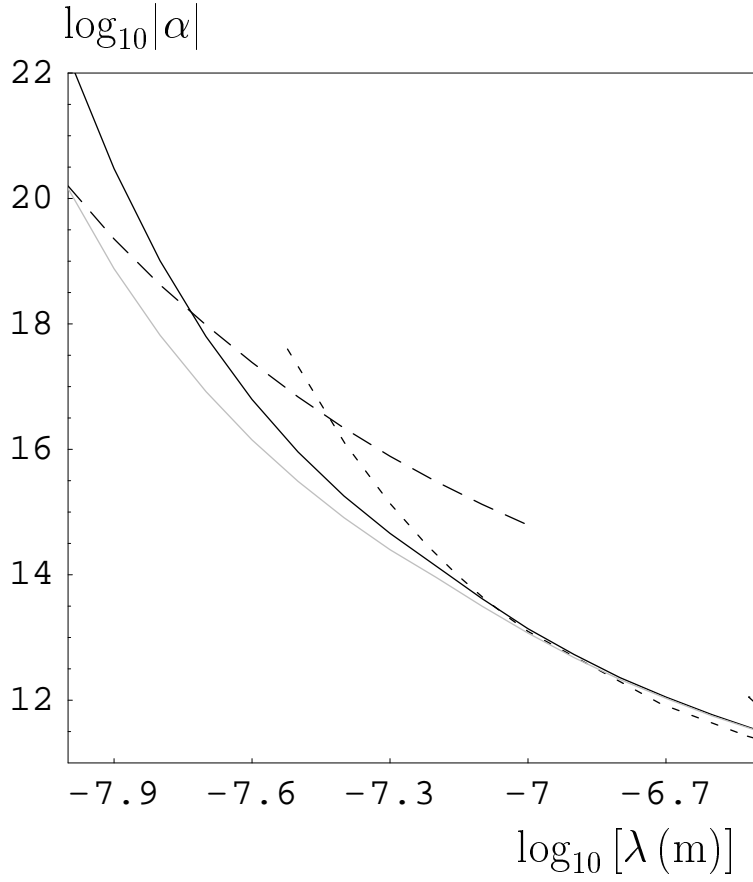


FIG. 3: Constraints on the parameters of Yukawa-type interaction from the experiment using a micromachined oscillator (the solid line), from the same experiment where the plane plate is replaced with the corrugated plate (the grey line), from measurements of the normal Casimir force by means of an atomic force microscope (the long-dashed line), and from the Casimir-less experiment (the short-dashed line). The allowed regions in the (λ, α) -plane lie beneath the lines.

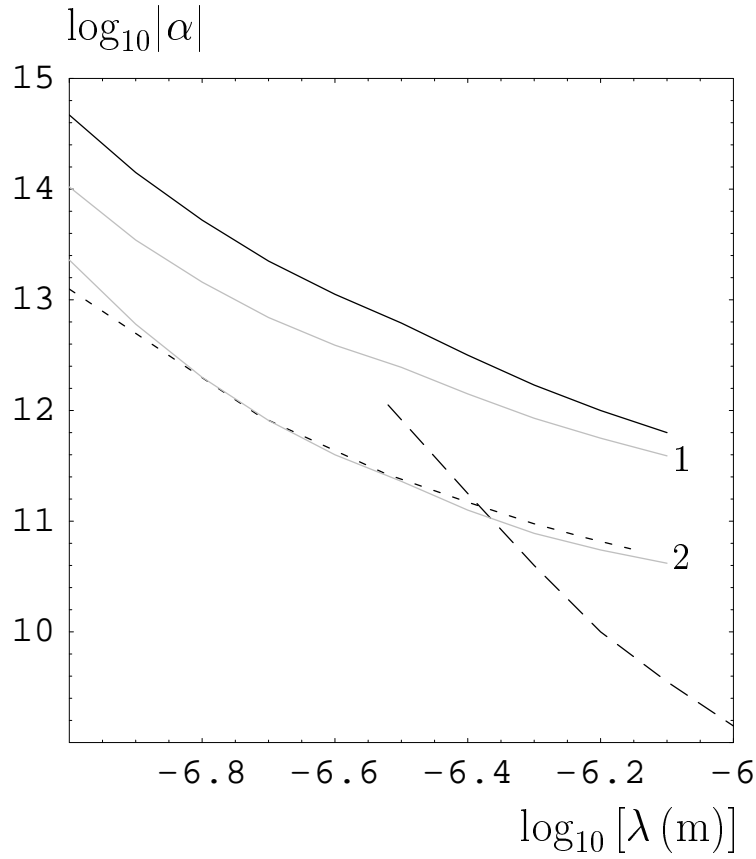


FIG. 4: Constraints on the parameters of Yukawa-type interaction from the experiment with two parallel plates (the solid line), from the same experiment with a Cr coating replaced with an Au coating of the same thickness (the grey line 1), from the same experiment with ten times thicker Au coating (the grey line 2), from the Casimir-less experiment (the short-dashed line), and from the measurement of the Casimir force by means of a torsion pendulum (the long-dashed line). The allowed regions in the (λ, α) -plane lie beneath the lines.

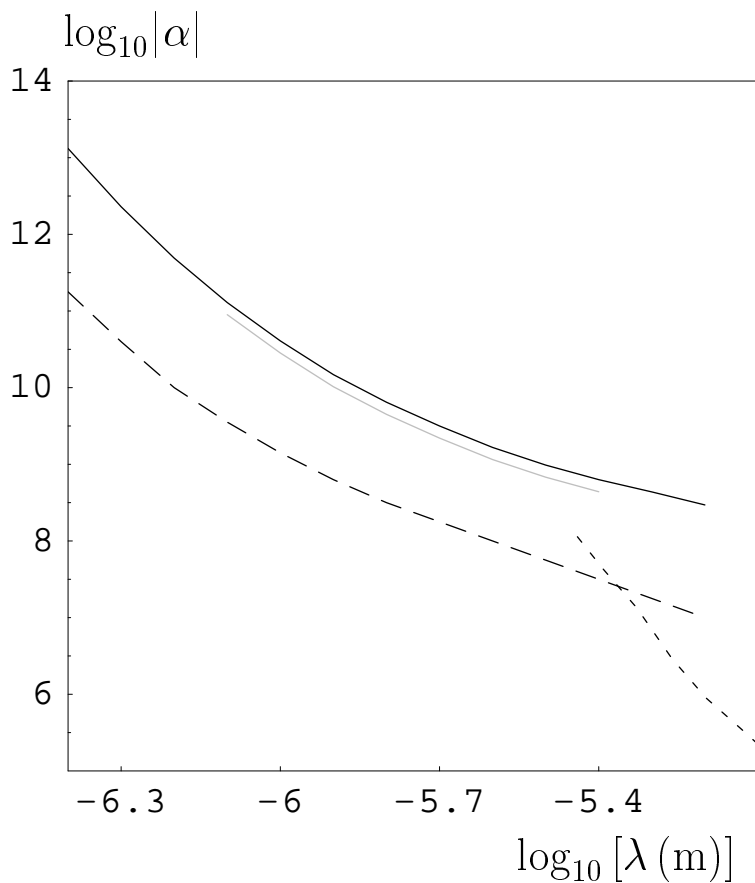


FIG. 5: Constraints on the parameters of Yukawa-type interaction from measurements of the Casimir-Polder force (the solid line), from the experiment using a torsion balance (the grey line), from the measurement of the Casimir force by means of a torsion pendulum (the long-dashed line), and from the gravitational experiment of Ref. [17] (the short-dashed line). The allowed regions in the (λ, α) -plane lie beneath the lines.